The Twenty-Fifth International Symposium on Artificial Life and Robotics 2020 (AROB 25th 2020),
The Fifth International Symposium on BioComplexity 2020 (ISBC 5th 2020),
B-Con Plaza, Beppu, Japan, January 22-24, 2020

Improvement of Force-sensorless Grinding with On-line Constraint Estimation

Kazuma Yamamoto[1], Mamoru Minami[1]

[1]Okayama University, Japan
(Tel: 81-086-252-1111)
[1]minami-m@cc.okayama-u.ac.jp

Abstract: This research aims to achieve a new grinding robot system that can grind an object into desired shape with force-sensorless control. In order to grind the target object into desired shape with sufficient accuracy, the hand of the robot arm has to generate desired constrained force immediately after the grindstone being contacted with the metal object to be ground. Based on the algebraic equation, we have proposed Constraint-Combined Force Controller, which has the ability to achieve the force control without time delay if the motors should ideally generate required torques without time delay. In order to give the system the ability to grind any working object into any shape, we focus on how to update the constraint condition in real time. Based on the above preparation we constructed a simulator to evaluate the proposed shape-grinding system, resulting in having proven the validity of our system to have the performance to adapt for grinding to desired-shape without force sensor and on-line estimation is performed by spline curve and quadratic function and the result is compared with bezier curve. As a result, it is best to use bezier curve for on-line estimation.

Keywords: force-sensorless grinding, robot, shape-grinding.

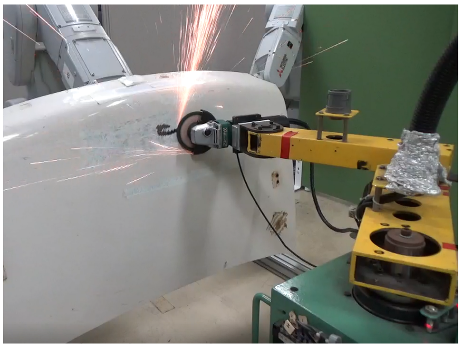

Fig. 1. Grinding robot

1 INTRODUCTION

Industrial robots are used for many purposes, especially as machining facilities. For example, there are welding, assembling and grinding operations. This research aims to achieve a new grinding robot system that can grind an object into desired shape with force-sensorless control in real experiment. Based on the analysis of the interaction between a manipulator's hand and a work-piece, a model representing the constrained dynamics of the robot is first discussed. Many researches have discussed force control methods of robots for constrained tasks. These control strategies use force sensors generally to obtain force information[1]-[3], where the reliability and accuracy are limited since the work-sites of the robot tend to be filled with noise and thermal disturbances, reducing the sensor's reliability. On top of this, force sensors could lead to the falling of the structure stiffness of manipulators, which is one of the most essential defects for manipulators executing grinding tasks. To solve these problems, some approaches that don't use force sensors have been presented[4]-[8]. In previous our research, we discussed about grinding task of robot that have disk grinder as an end-effector. Our grinding robot is 2-link SCARA manipulator. The contact process of the grinder can be just thought as non-dynamical process but a kinematical one, so the prerequisite that there is no motion occurred in vertical direction to the surface to be ground could be justifiable. Therefore, equation of motion to describe constrained vertical process of the grinder contacting to the work-piece is represented by an algebraic equation. Based on this algebraic equation, we have proposed Constraint-Combined Force Controller[11], [12], which has the ability to achieve the force control without time delay if the motors ideally should generate required torques without time delay, where force error will not be affected by the dynamical motion along to the surface on which the grinder can move[11], [12]. Our Constraint-Combined force/position control method without using tactile sensor can be thought to be essentially different from methods proposed so far. Constraint-Combined Force Controller can compute the input torques to achieve desired force/position by using posture and angular velocity of the robot and frictional force. In this presentation, we estimate the object's surface using the grinder as a touch sensor. In order to give the system to grind any working object into any shape, we focus on how to update the constraint condition in real time. Based on the above preparation we constructed a simulator to evaluate the proposed shape-grinding system, resulting in having proven the validity of our system to have the performance to adapt for grinding to desired-shape without force sensor. On-line estimation is performed by bezier curve and quadratic function and the result is compared with spline curve.

2 MODELLING OF CONTACT DYNAMICS

In this paper,the end-point of the grinding manipulator shown in Fig. 1 is in contact with the constrained surface. Constraint condition C is a scalar function of the constraint, and is expressed as an algebraic equation of constraints as

$$C(\boldsymbol{r}(\boldsymbol{q})) = 0 \tag{1}$$

where $\boldsymbol{r}(m \times 1)$ is the position vector from origin of coordinates to tip of grinding wheel and $\boldsymbol{q}(n \times 1)$ is joint angles. The grinder set at the robot's hand is in contact with the material that is to be ground. The equation of motion of grinding robot is modelled as following Eq.(2)[11],[12],

$$\boldsymbol{M}(\boldsymbol{q})\ddot{\boldsymbol{q}} + \boldsymbol{h}(\boldsymbol{q}, \dot{\boldsymbol{q}}) + \boldsymbol{g}(\boldsymbol{q}) + \boldsymbol{D}\dot{\boldsymbol{q}} = \boldsymbol{\tau} + {\boldsymbol{J}_C}^T f_n - {\boldsymbol{J}_R}^T f_t \tag{2}$$

$${\boldsymbol{J}_C}^T = \left(\frac{\partial \boldsymbol{r}}{\partial \boldsymbol{q}}\right)^T \frac{\left(\dfrac{\partial C}{\partial \boldsymbol{r}}\right)^T}{\left\|\dfrac{\partial C}{\partial \boldsymbol{r}}\right\|} \tag{3}$$

$${\boldsymbol{J}_R}^T = \left(\frac{\partial \boldsymbol{r}}{\partial \boldsymbol{q}}\right)^T \frac{\dot{\boldsymbol{r}}}{\|\dot{\boldsymbol{r}}\|} \tag{4}$$

where $\boldsymbol{M}$ is a $n \times n$ matrix, $\boldsymbol{h}$ is centrifugal and coriolis force vector, $\boldsymbol{D}$ is viscous friction coefficient matrix, $\boldsymbol{g}$ is gravity vector. f_n is the constrained force associated with C and f_t is the tangential disturbance force caused by grinding. Moreover, ${\boldsymbol{J}_C}^T$ is time-varying coefficient vector translating f_n into each joint disturbance torque and ${\boldsymbol{J}_R}^T$ is time-varying coefficient vector transmitting the tangential disturbance force f_t to joint disturbance torque. The equation represented by Eq.(2) must follow the constraint condition given by Eq.(1) during the contacting motion of grinding. Differentiating Eq.(1) by time twice, we have the following relation among $\boldsymbol{q}$, $\dot{\boldsymbol{q}}$ and $\ddot{\boldsymbol{q}}$ that should be maintained during contacting motion with the work-piece to be ground,

$$\left[\frac{\partial}{\partial \boldsymbol{q}}\left(\frac{\partial C}{\partial \boldsymbol{q}}\right)\dot{\boldsymbol{q}}\right]\dot{\boldsymbol{q}} + \left(\frac{\partial C}{\partial \boldsymbol{q}}\right)\ddot{\boldsymbol{q}} = 0 \tag{5}$$

Above constraint condition represents an algebraic condition of $\ddot{\boldsymbol{q}}$ that have to be determined dependently on $\boldsymbol{q}$ and $\dot{\boldsymbol{q}}$.

Putting $\ddot{\boldsymbol{q}}$ in Eq.(5) into $\ddot{\boldsymbol{q}}$ in Eq.(2) to be determined identically so as the solution of $\boldsymbol{q}$ and $\dot{\boldsymbol{q}}$ of Eq.(2) to comply simultaneously with the constraint condition Eq.(5), the solution $\ddot{\boldsymbol{q}}$ and f_n could be uniquely determined. The following Eq.(6) is the resulted solution of f_n [11],[12],

$$f_n = a(\boldsymbol{q}, \dot{\boldsymbol{q}}) + \boldsymbol{B}(\boldsymbol{q}){\boldsymbol{J}_R}^T f_t - \boldsymbol{B}(\boldsymbol{q})\boldsymbol{\tau} \tag{6}$$

Where m_c, $a(\boldsymbol{q}, \dot{\boldsymbol{q}})$ and $\boldsymbol{B}(\boldsymbol{q})$ are

$$m_c \triangleq \left(\frac{\partial C}{\partial \boldsymbol{q}}\right)\boldsymbol{M}^{-1}\left(\frac{\partial C}{\partial \boldsymbol{q}}\right)^T \tag{7}$$

$$\begin{aligned} a(\boldsymbol{q}, \dot{\boldsymbol{q}}) \triangleq {m_c}^{-1}\left\|\frac{\partial C}{\partial \boldsymbol{r}}\right\|\Bigg\{&-\left[\frac{\partial}{\partial \boldsymbol{q}}\left(\frac{\partial C}{\partial \boldsymbol{q}}\right)\dot{\boldsymbol{q}}\right]\dot{\boldsymbol{q}} \\ &+\left(\frac{\partial C}{\partial \boldsymbol{q}}\right)\boldsymbol{M}^{-1}(\boldsymbol{h}+\boldsymbol{g})\Bigg\} \end{aligned} \tag{8}$$

$$\boldsymbol{B}(\boldsymbol{q}) \triangleq {m_c}^{-1}\left\|\frac{\partial C}{\partial \boldsymbol{r}}\right\|\left\{\left(\frac{\partial C}{\partial \boldsymbol{q}}\right)\boldsymbol{M}^{-1}\right\} \tag{9}$$

Substituting Eq.(6) into Eq.(2), the equation of motion of the constrained robot dynamics (as $f_n > 0$) can be rewritten as

$$\begin{aligned} &\boldsymbol{M}(\boldsymbol{q})\ddot{\boldsymbol{q}} + \boldsymbol{h}(\boldsymbol{q}, \dot{\boldsymbol{q}}) + \boldsymbol{g}(\boldsymbol{q}) = {\boldsymbol{J}_C}^T a(\boldsymbol{q}, \dot{\boldsymbol{q}}) \\ &+(\boldsymbol{I} - {\boldsymbol{J}_C}^T\boldsymbol{B})\boldsymbol{\tau} + ({\boldsymbol{J}_C}^T\boldsymbol{B} - \boldsymbol{I}){\boldsymbol{J}_R}^T f_t \end{aligned} \tag{10}$$

Solutions of above dynamic equation always satisfy the constrained condition, then accordingly $\boldsymbol{q}$ satisfies Eq.(1).

3 CONSTRAINT-COMBINED FORCE/POSITION CONTROL METHOD

In the following discussions of grinding task, we assume that $m = 2$, $n = 2$, C is scalar function, since we use two link manipulator as a experimental device. Putting the above assumptions and Eq.(6) into consideration we can claim that there is a redundancy of the number of the constrained force, one, against the number of the input torque $\boldsymbol{\tau} = [\tau_1, \tau_2]$. This condition is much similar to the kinematical redundancy. Based on the above argument and assume that, the parameters of the Eq.(6) are known and its state variables could be measured, and $a(\boldsymbol{q}, \dot{\boldsymbol{q}})$ and $\boldsymbol{B}(\boldsymbol{q})$ could be calculated correctly, which means that the constraint condition $C = 0$ be prescribed or measured correctly. As a result, a control law is derived from Eq.(6) and can be expressed as

$$\begin{aligned} \boldsymbol{\tau} = -\boldsymbol{B}^+(\boldsymbol{q})\{f_{nd} - a(\boldsymbol{q}, \dot{\boldsymbol{q}}) - \boldsymbol{B}(\boldsymbol{q}){\boldsymbol{J}_R}^T f_t\} \\ +\{\boldsymbol{I} - \boldsymbol{B}^+(\boldsymbol{q})\boldsymbol{B}(\boldsymbol{q})\}\boldsymbol{k}, \end{aligned} \tag{11}$$

where $\boldsymbol{I}$ is a 2×2 identity matrix, f_{nd} is the desired constrained forces, $\boldsymbol{B}(\boldsymbol{q})$ is defined as Eq.(9) and $\boldsymbol{B}^+(\boldsymbol{q})$ is the pseudoinverse matrix of it, $a(\boldsymbol{q}, \dot{\boldsymbol{q}})$ is defined as Eq. (8) and $\boldsymbol{k}$ is an arbitrary vector used for hand position control, which is given as

$$\boldsymbol{k} = \left(\frac{\partial \boldsymbol{r}}{\partial \boldsymbol{q}}\right)^T \{\boldsymbol{K}_P(\boldsymbol{r}_d - \boldsymbol{r}) + \boldsymbol{K}_V(\dot{\boldsymbol{r}}_d - \dot{\boldsymbol{r}})\}, \tag{12}$$

The Twenty-Fifth International Symposium on Artificial Life and Robotics 2020 (AROB 25th 2020),
The Fifth International Symposium on BioComplexity 2020 (ISBC 5th 2020),
B-Con Plaza, Beppu, Japan, January 22-24, 2020

where $\boldsymbol{K}_P$ and $\boldsymbol{K}_V$ are gain matrices for position and the velocity control. The position and velocity control is conducted through the redundant degree of range space of $\boldsymbol{B}$, that is null space of $\boldsymbol{B}$, specifically $\{\boldsymbol{I}-\boldsymbol{B}^+\boldsymbol{B}\}$. $\boldsymbol{r}_d$ is the desired position vector of the end-effector along to the constrained surface and $\boldsymbol{r}$ is the real position vector on it. $\boldsymbol{K}_P$ and $\boldsymbol{K}_V$ is needed to be set with a reasonable value, otherwise high-frequency oscillation of position error may appear. The controller presented by Eq.(11) and Eq.(12) assumes that the constraint condition $C=0$ be known precisely even though the grinding operation is a task to change the constraint condition. We need to observe time-varying constraint condition in real time using grinding tip as a touch sensor. The time-varying condition is estimated as an approximate constrained function by position of the manipulator hand, which is based on the estimated constrained surface location. The estimated condition is donated by $\hat{C}=0$(in this paper, 'ˆ' means the situation of unknown constraint condition). Hence, $a(\boldsymbol{q},\dot{\boldsymbol{q}})$ and $\boldsymbol{B}(\boldsymbol{q})$ including $\hat{C}$ are changed to $\hat{a}(\boldsymbol{q},\dot{\boldsymbol{q}})$ and $\hat{\boldsymbol{B}}(\boldsymbol{q})$ as shown in Eq.(13) and Eq.(14). They were used in the later experiments of the unknown constrained condition. As a result, a controller based on the estimated constrained condition is given as Eq.(15) and Eq.(16).

$$\begin{aligned}\hat{a}(\boldsymbol{q},\dot{\boldsymbol{q}}) \;\triangleq\; & {m_c}^{-1}\left\|\frac{\partial\hat{C}}{\partial\boldsymbol{r}}\right\|\left\{-\dot{\boldsymbol{q}}^T\left[\frac{\partial}{\partial\boldsymbol{q}}\left(\frac{\partial\hat{C}}{\partial\boldsymbol{q}}\right)\dot{\boldsymbol{q}}\right]\right.\\ & + \left.\left(\frac{\partial\hat{C}}{\partial\boldsymbol{q}}\right)\boldsymbol{M}^{-1}(\boldsymbol{h}+\boldsymbol{g})\right\} \qquad (13)\end{aligned}$$

$$\hat{\boldsymbol{B}}(\boldsymbol{q}) \;\triangleq\; {m_c}^{-1}\left\|\frac{\partial\hat{C}}{\partial\boldsymbol{r}}\right\|\left\{\left(\frac{\partial\hat{C}}{\partial\boldsymbol{q}}\right)\boldsymbol{M}^{-1}\right\} \qquad (14)$$

$$\begin{aligned}\hat{\boldsymbol{\tau}} = -\hat{\boldsymbol{B}}^+(\boldsymbol{q})\{f_{nd}-\hat{a}(\boldsymbol{q},\dot{\boldsymbol{q}})-\hat{\boldsymbol{B}}(\boldsymbol{q})\boldsymbol{J}_R{}^T f_t\}\\ +\{\boldsymbol{I}-\hat{\boldsymbol{B}}^+(\boldsymbol{q})\hat{\boldsymbol{B}}(\boldsymbol{q})\}\hat{\boldsymbol{k}} \qquad (15)\end{aligned}$$

$$\hat{\boldsymbol{k}} = \left(\frac{\partial\boldsymbol{r}}{\partial\boldsymbol{q}}\right)^T\{\boldsymbol{K}_P(\hat{\boldsymbol{r}}_d-\boldsymbol{r})+\boldsymbol{K}_D(\dot{\hat{\boldsymbol{r}}}_d-\dot{\boldsymbol{r}})\} \qquad (16)$$

4 ON-LINE ESTIMATION METHOD

In the preceding section, shape-grinding method is solved in our research. But how to estimate the unknown constraint surface is the key point. Here, an unknown constrained condition is assumed as in the following.

1 The end-point position of the manipulator during the grinding task can be surely measured and updated.

2 The grinding task is defined in the $x-y$ plane.

3 When beginning to work, the initial condition of the end-effector is known and it has touched the work object.

Like the situation shown in Fig. 2, the grinding surface is not a simple straight line or some curve line which can be defined and expressed by some certain curve equation. Grinding robot has no idea since input torque cannot be derived without constraint condition. To solve this problem, we consider that some kind of on-line estimation function is utilized to imitate the unknown grinding surface, to obtain an unknown constraint condition, which can be used to calculate the input torque. Therefore, now let us take a look at Fig. 2. Point(x_{i-1},y_{i-1}) and Point(x_i,y_i) are known because they are just ground by the grinder and the information of points (x_{i-1},y_{i-1}) and (x_i,y_i) can be derived through the position of robot's end-effector. In this paper, for building an estimation function, spline function and function and bezier function are used.

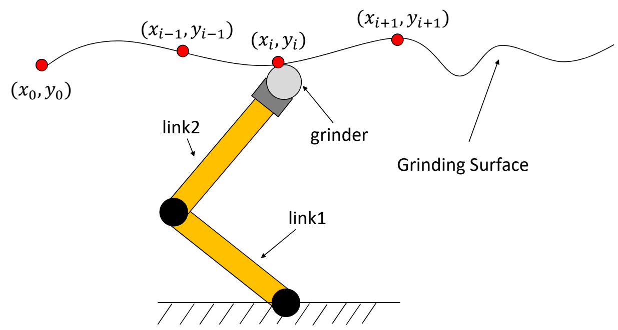

Fig. 2. On-line estimation model

4.1 A quadratic spline curve

A quadratic spline function is generated by two points and is expressed by the expression

$$S(x_i)=\alpha_i(x_i-x_{i-1})^2+\beta_i(x_i-x_{i-1})+\gamma_i \qquad (17)$$

Firstly, let $S_i(x_i)$ satisfy the following conditions shown in Fig. 3.

(A)Go through the two ends of interval

$$y_{i-1}=S_i(x_{i-1}) \qquad (18)$$

$$y_i=S_i(x_i) \qquad (19)$$

(B)First-order differential of the spline polynomials is equal at the end-point of the adjoined function.

$$S'_{i+1}(x_i)=S'_i(x_i) \qquad (20)$$

From the relation among (17)-(20), we can obtain:

$$\gamma_i=y_{i-1} \qquad (21)$$

$$\beta_{i+1}=2u_i-\beta_i \qquad (22)$$

$$\alpha_i=\frac{\beta_{i+1}-\beta_i}{2h_i} \qquad (23)$$

Where $h_i=x_i-x_{i-1}$, $u_i=\frac{y_i-y_{i-1}}{h_i}$.

The Twenty-Fifth International Symposium on Artificial Life and Robotics 2020 (AROB 25th 2020),
The Fifth International Symposium on BioComplexity 2020 (ISBC 5th 2020),
B-Con Plaza, Beppu, Japan, January 22-24, 2020

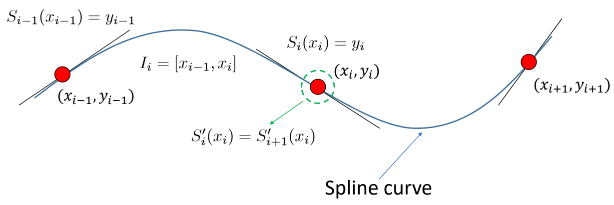

Fig. 3. Generation of quadratic spline curve

4.2 A quadratic function curve

A quadratic function is generated by three points and is expressed by the expression

$$f(x_i) = \alpha_i x_i^2 + \beta_i x_i + \gamma_i \tag{24}$$

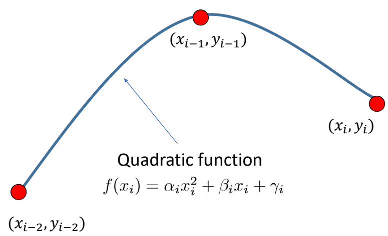

Fig. 4. Generation of quadratic function

$$\alpha_i = \frac{(x_i - x_{i-2})(y_{i-1} - y_{i-2}) - (y_i - y_{i-2})(x_{i-1} - x_{i-2})}{(x_i - x_{i-2})(x_{i-1} - x_{i-2})(x_{i-1} - x_i)} \tag{25}$$

$$\begin{aligned}\beta_i = \{&(x_{i-1} - x_{i-2})(y_i - y_{i-2})(x_{i-1} + x_{i-2}) \\ &-(y_{i-1} - y_{i-2})(x_i - x_{i-2})(x_i + x_{i-2})\} \\ &/(x_i - x_{i-2})(x_{i-1} - x_{i-2})(x_{i-1} - x_i)\end{aligned} \tag{26}$$

$$\gamma_i = y_{i-2} - \alpha_i x_{i-2}^2 - \beta_i x_{i-2} \tag{27}$$

4.3 A quadratic bezier curve

A quadratic bezier function is generated by three points and is expressed by the expression

$$\boldsymbol{b}(t) = \sum_{i=0}^{2} B_i^n(t) \boldsymbol{b}_i \tag{28}$$

Where $B_i^n(t) = {}_nC_i t^i (1-t)^{n-i}$. As shown in Fig.5, the bezier curve is generated by repeatedly acquiring the internally dividing point of the line segment from given points. bezier curve passes through the start and end points, but does not pass through the midpoint.

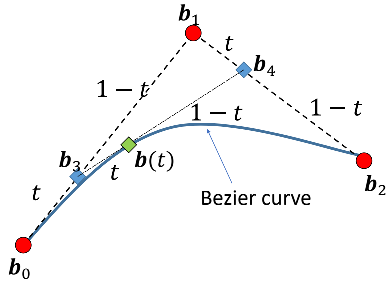

Fig. 5. Generation of quadratic bezier curve

5 EXPERIMENT

The experimental equipment is shown in Fig.6. In this experiment, we use grinding robot and an articulated robot(RV-20F) for grinding. A car bonnet is used as a target for this experiments. The target appearance is shown in Fig.7. We conducted grinding experiment with on-line constraint estimation by spline curve and quadratic function and bezier curve. For experimental condition, grinding time is set to 10[s], grinding area is x[0.0,15.0][mm].

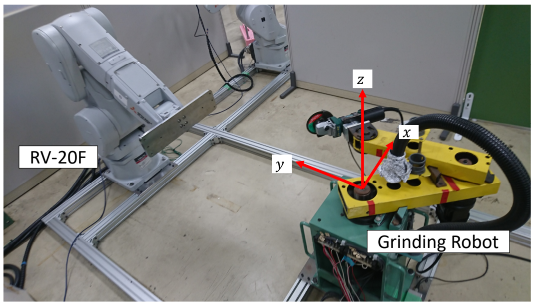

Fig. 6. Experiment environment

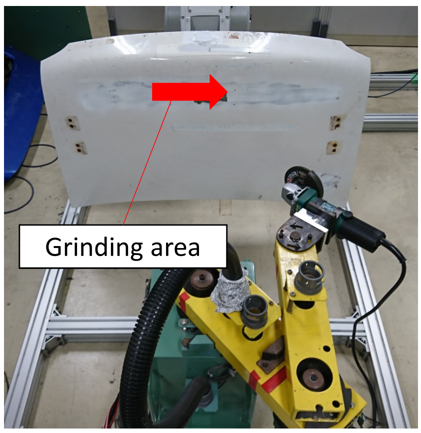

Fig. 7. Grinding area

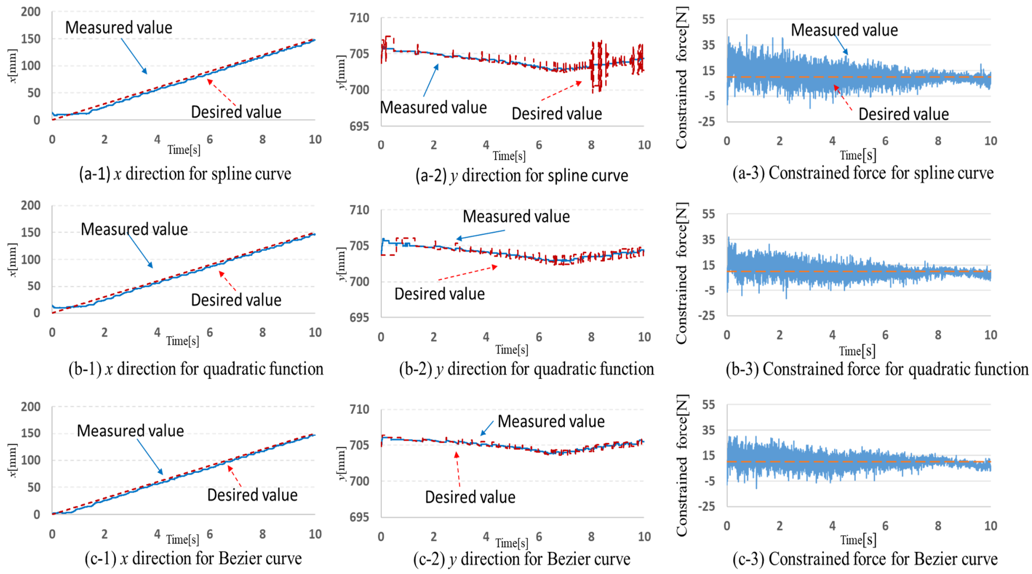

Fig. 8. Experiment result of x direction, y direction and constrained force for each approximation curve

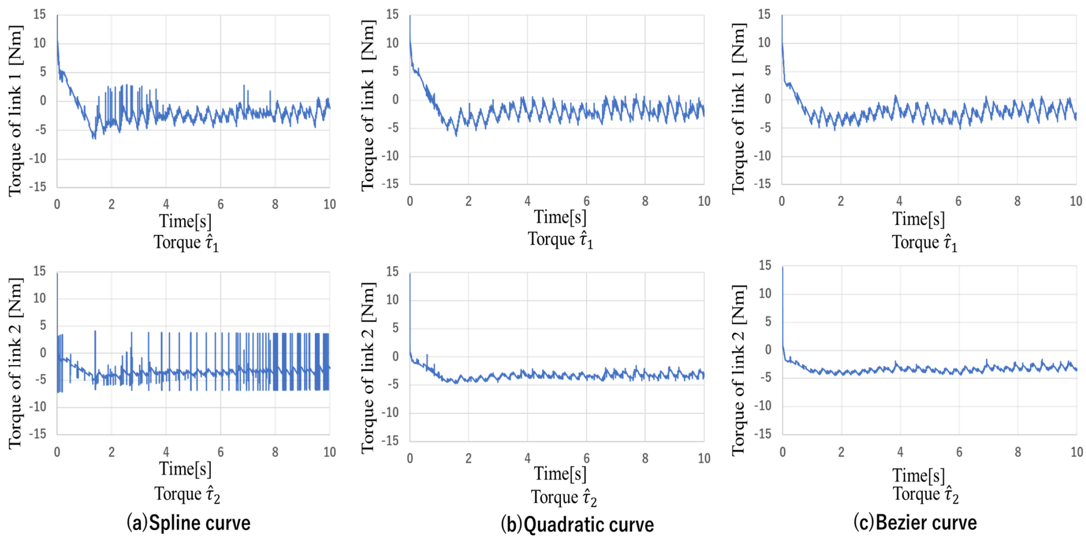

Fig. 9. Result of torque $\hat{\tau}_{1,2}$ by each curves

Figure 8 shows the experimental result of grinding operation in x direction, y direction and constrained force for each carve approximation. For Fig. 8, (a-1)-(a-3) show the result of spline curve approximation, (b-1)-(b-3) show the result of quadratic function approximation, and (c-1)-(c-3) show the result of bezier curve approximation. For Fig. 8 (a-1), (b-1) and (c-1) shows x direction. The steady-state error occur about 2[mm] among measured value and desired value for each curve approximation. As for the result of on-line constraint estimation, experimental result is compared with error among measured value and desired value in y direction. The dotted line shows desired value generated by each curve approximation and the solid line shows the hand trajectory of grinding robot. In Fig. 8, the result of spline curve approximation shows that large errors generated. In the method of quadratic function approximation, errors of 1[mm] or more occur. However the result of bezier curve approximation shows that errors did not occur more than 1[mm]. In this experiment, constrained force was measured by force sensor attached to grinding robot. The force sensor is used only to measure constrained force and not to control the grinding robot. When compared bezier curve with spline curve in constrained force, amplitude of vibration in the result of bezier curve is smaller than spline curve. Figure 9 shows change of torque generated in each joint by spline curve, quadratic function and bezier curve, respectively. As shown in Fig. 9, amplitude of vibration for torque generated in spline curve approximation is bigger than bezier curve and quadratic function. For this experiment result, the estimation result for y direction by each approximation curves are related to the size of the amplitude vibration.

Figure 10, Figure 11 and Figure 12 shows, in each curve approximation, experiment result of y direction (a) for 3.2 seconds to 3.6 seconds and (b) and (c) show the calculated torque of each joint in the grinding joint for 3.2 seconds to 3.6 seconds. For each experiment result of y direction (a), errors among measured value and desired value generated in 3.4 seconds by on-line estimation for each curve approximation. In this time, the vibration of the calculated torque for each curve generated corresponding to experiment results of y direction in 3.4 seconds. As a result, the result of shape estimation affect torque control for each joint.

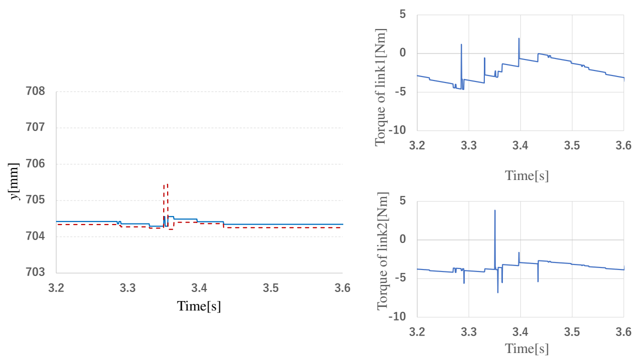

Fig. 10. Result of y position and torque $\hat{\tau}_{1,2}$ by spline curve from 3.2[s] to 3.6[s]

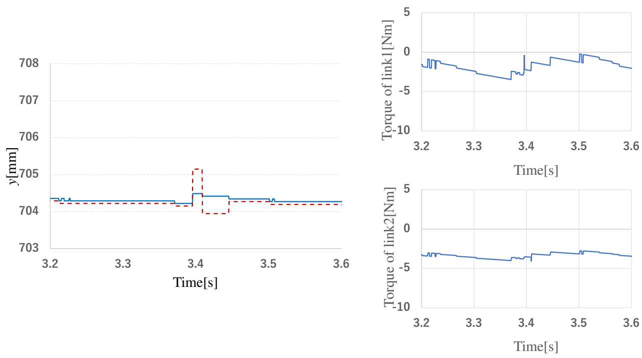

Fig. 11. Result of y position and torque $\hat{\tau}_{1,2}$ by quadratic function from 3.2[s] to 3.6[s]

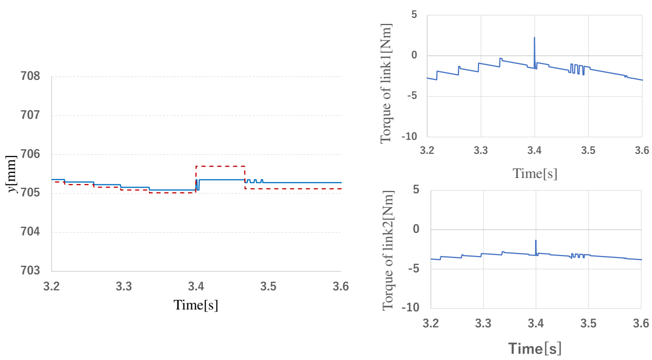

Fig. 12. Result of y position and torque $\hat{\tau}_{1,2}$ by bezier curve from 3.2[s] to 3.6[s]

6 CONCLUSION

In order to verify the feature of the proposed force-sensorless force/position hybrid control, the experiments of the proposed force/position hybrid control method were executed for three approximation curves. From the experimental results, so generated errors among measured value and desired value affect torque control for each approximation curve, it was shown that it is better to use bezier curve that generated the smallest errors of three approximation curve.

REFERENCES

[1] M.H.Raibert and J.J.Craig: Hybrid Position/Force Control of Manipulators, Trans. of the ASME, J. of Dynamic Systems, Measurement and Control, Vol.102, pp.126-133, June, 1981.

[2] S. Arimoto, Mechanics and Control of Robot(in Japanese), Asakura Publishing Co., Ltd., Tokyo, Japan, 1990.

[3] T. Yoshikawa: Dynamic Hybrid Position/Force control of Robot Manipulators — Description of Hand Constraints and Calculation of Joint Driving Force, IEEE J. on Robotics and Automation, Vol.RA-3, No.5, pp.386-392, 1987.

[4] L. Whitcomb, S. Arimoto, T. Naniwa and F. Osaki, Experiments in Adaptive Model-Based Force Control, IEEE Control Systems Society, Vol.16, No.1, pp.49-57, 1996.

[5] Z. X. Peng and N. Adachi: Position and Force Control of Manipulators without Using Force Sensors(in Japanese), Trans. of JSME(C), Vol.57, No.537, pp.1625-1630, 1991.

[6] Jaydeep. Roy and Louis L. Whitcomb: Adaptive Force Control of Position/Velocity Controlled Robots: Theory and Experiment, IEEE Transactions on Robotics and Automation, Vol.18, No.2, April, 2002.

[7] B. Siciliano, L. Villani, Robot Force Control, Kluwer Academic Publishers, U.K., 1999.

[8] C. Natale, Interaction Control of Robot Manipulators, Springer Tracts in Advanced Robotics, Germany, 2003.

[9] N. Hogan: Impedance control: An approach to manipulation: Part 1-Theory, J.Dynamic Syst., Measurement Contr., Vol.107, pp.1-7, Mar, 1985.

[10] Hooshang Hemami and Bostwick F. Wyman: Modeling and Control of Constrained Dynamic Systems with Application to Biped Locomotion in the Frontal Plane, IEEE Trans. on Automatic Control, Vol.AC-24, No.4, pp.526-535, 1979.

[11] Takeshi Ikeda, Mamoru Minami, Position/Force Control of a Manipulator by Using an Algebraic Relation and Evaluations by Experiments, The 2003 IEEE/ASME Int. Conf. on Advanced Intelligent Mechatronics (AIM2003), Proceeding CD-ROM paper No.159, 503-508, 2003

[12] Takeshi Ikeda and Mamoru Minami: Research of Grinding Robot without Force Sensor by Using Algebraic Equation(in Japanese), Transactions of the Japan Society of Mechanical Engineers(C), Vol.71, No.702, pp.270-277, 2005.